JIPB Journal of Integrative Plant Biology

Research Article
https://doi.org/10.1111/jipb.13927

Harnessing Green Revolution genes to optimize tomato production efficiency for vertical farming

Xuchen Yu[1,2,3†], Zuoyao Li[4†], Yongfang Yang[1,2†], Shujia Li[1,2], Yezi Lu[1,2,3], Yang Li[5], Xinyu Zhang[1,2,3], Fan Chen[1,6*] and Cao Xu[1,2,3*]

1. Key Laboratory of Seed Innovation, National Center for Plant Gene Research (Beijing), Institute of Genetics and Developmental Biology, Chinese Academy of Sciences, Beijing 100101, China
2. CAS–JIC Centre of Excellence for Plant and Microbial Science, Institute of Genetics and Developmental Biology, Chinese Academy of Sciences, Beijing 100101, China
3. College of Advanced Agricultural Sciences, University of Chinese Academy of Sciences, Beijing 100049, China
4. College of Tropical Crops, Hainan University, Haikou 570228, China
5. Plant Factory R&D Center, Institute of Botany, Chinese Academy of Sciences, Beijing 100093, China
6. Yazhouwan National Laboratory, Sanya 572024, China

†These authors contributed equally to this article.

*Correspondences: Fan Chen (fchen@genetics.ac.cn); Cao Xu (caoxu@genetics.ac.cn; Dr. Xu is fully responsible for the distribution of all materials associated with this article)

Xuchen Yu

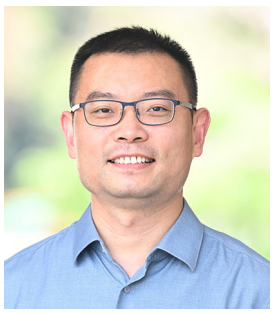

Cao Xu

ABSTRACT

Vertical farming offers significant potential to tackle global challenges like urbanization, food security, and climate change. However, its widespread adoption is hindered by high costs, substantial energy demands, and thus low production efficiency. The limited range of economically viable crops further compounds these challenges. Beyond advancing infrastructure, rapidly developing crop cultivars tailored for vertical farming (VF) are essential to enhancing production efficiency. The gibberellin biosynthesis genes *GA20-oxidase* fueled the Green Revolution in cereals, while the anti-florigen genes *SELF-PRUNING* (*SP*) and *SELF-PRUNING 5G* (*SP5G*) revolutionized tomato production. Here, we engineer tomato germplasm optimized for VF by leveraging genome editing to integrate Green Revolution gene homologs and anti-florigen genes. Knocking out the tomato *SlGA20ox1* gene, but not *SlGA20ox2*, results in a promising VF-suitable plant architecture featuring short stems and a compact canopy. When cultivated in a commercial vertical farm with multi-layered, LED-equipped automated hydroponic growth systems, *slga20ox1* mutants saved space occupation by 75%, achieving a 38%–69% fruit yield increase with higher planting density, less space occupation, and lower lighting power consumption. Stacking *SlGA20ox1* with *SP* and *SP5G* genes created a more compact plant architecture with accelerated flowering and synchronized fruit ripening. In commercial vertical farms, the *sp sp5g slga20ox1* triple mutant reduced space occupation by 85%, shortened the harvest cycle by 16% and increased effective yield by 180%, significantly enhancing production efficiency. Our study demonstrates the potential of integrating agriculture practice-validated genes to rapidly develop tomato cultivars tailored for VF, providing a proof-of-concept for leveraging genome editing to boost production efficiency in VF.

Keywords: CRISPR/Cas9, GA20ox, Green Revolution, plant architecture, tomato, vertical farming

Yu, X., Li, Z., Yang, Y., Li, S., Lu, Y., Li, Y., Zhang, X., Chen, F., and Xu, C. (2025). Harnessing Green Revolution genes to optimize tomato production efficiency for vertical farming. J. Integr. Plant Biol. **00:** 1–15.

INTRODUCTION

The challenges posed by global climate change, declining land quality, water scarcity and population growth pose significant threats to traditional agricultural production and food security (Muluneh, 2021; Mahadevan et al., 2024). In recent years, controlled environment agriculture, also known as vertical farming (VF) has demonstrated considerable potential in addressing these pressing agricultural issues (Kwon et al., 2020; Zhang et al., 2022; Zhu and Marcelis, 2023). Compared with traditional agricultural models, VF possesses the capability to exercise intelligent control over a range of environmental factors within a closed plant production system, including lighting, temperature, humidity, and carbon dioxide levels. This provides a stable and controlled environment that is not constrained by climate or geography, while achieving high space efficiency, revolutionary water conservation and short supply chains (Figure 1A) (Kozai and Niu, 2016; van Delden et al., 2021). Therefore, VF has the potential to play a crucial role in the next agricultural revolution and in ensuring global food security.

However, production efficiency, which encompasses resource use and sustainability, is a critical constraint to VF development. The primary challenges include high initial capital investments for infrastructure (e.g., multi-tier cultivation systems and environmental control equipment), excessive energy consumption driven by continuous power demands (lighting, climate regulation, etc.), which substantially escalate operational costs, and limited crop diversity, with only a narrow range of economically viable crops (primarily leafy greens and herbs) currently adaptable to vertical systems (Figure 1A) (Kozai and Niu, 2016; van Delden et al., 2021). Additionally, even if artificial intelligence (AI) systems are used to optimize resource inputs and enhance production efficiency, the limited adaptability of crops to VF modules may hinder these efforts (Rathor et al., 2024). Therefore, to ensure the high productive efficiency of crops, it is imperative to accelerate the genetic gain of crops specifically optimized for VF systems (Figure 1B), thereby enhancing resource-use efficiency and boosting productivity per unit of energy input.

The Green Revolution was a typical event in agricultural upgrading that adapted crops to advanced productivity through breeding. Prior to this time, fertilizers provided unprecedented nutrient inputs to crops, and harvesters greatly improved harvesting efficiency, but tall crop cultivars were easily lodging over at high fertilizer levels, which in turn resulted in severe yield losses, as overly tall plants were not conducive to mechanized harvesting. The outdated cultivars were mismatched with advanced productivity such as fertilizers and harvesters (Hedden, 2003). Similar to this historical dilemma, the mismatch between crop cultivars and VF has also limited the development process of VF. During the Green Revolution, the lodging resistance and yields of wheat (*Triticum aestivum*) and rice (*Oryza sativa*) significantly increased due to the introduction of dwarfing traits into the plants. Now, research has revealed that the genes responsible for these traits interfere with the biosynthesis or response of the plant hormone gibberellin (GA) (Peng et al., 1999; Sasaki et al., 2002; Hedden, 2003). Gibberellins, a class of phytohormones, regulate diverse physiological processes across all developmental stages of plants. The most well characterized role of GAs is to vegetative growth through mediating stem elongation and leaf expansion, which synergistically enhance light capture and biomass accumulation (Yamaguchi, 2008). Gibberellin-deficient mutants typically display compact, dark green leaves and significantly inhibited internode elongation (Richards et al., 2001; Sakamoto et al., 2004).

The Green Revolution gene *SEMIDWARF-1* (*SD1*) in rice encodes the key enzyme GA20 oxidase (OsGA20ox2) in the GA biosynthetic pathway (Sasaki et al., 2002). Mutation of the *OsGA20ox2* gene leads to the accumulation of DELLA proteins in rice, inhibiting GA signal transduction and resulting in dwarfism in the plants. Gibberellin 20-oxidase, a 2-oxoglutarate-dependent dioxygenase, is the rate-limiting enzyme for the production of active GA and plays a vital regulatory role in modulating GA levels in plants (Coles et al., 1999). It has been revealed that GA 20-oxidase is encoded by multigene families, the members of which exhibit distinct positional and temporal expression patterns (Sakamoto et al., 2004). In rice, variation in the activity of *OsGA20ox1* and *OsGA20ox3*, two paralogs of *OsGA20ox2*, confers changes in height and panicle architecture, demonstrating that both these genes contribute to stem elongation in rice (Oikawa et al., 2004; Qin et al., 2013). Analogous to previous findings, CRISPR/Cas9-mediated knockout of the *GA20ox3* gene in maize (*Zea mays*) triggered a substantial decline in bioactive GA_1 and GA_4 concentrations with the semi-dwarf phenotype (Zhang et al., 2020). Similarly, wheat *Ga20ox2* loss-of-function mutants demonstrated a 58%–64% depletion in GA_1 accumulation coupled with a 12%–32% reduction in plant height compared with isogenic wild-type (WT) lines (Ndreca et al., 2024). In addition to cereal crops, the function of GA20ox genes is also conserved in Solanaceae crops. Silencing the *GA20ox1* gene in potato (*Solanum tuberosum*) resulted in shortened stems and reduced internode length (Carrera et al., 2000), while suppression of GA20ox members in tomato (*Solanum lycopersicum*) had similarly shown short stems and reduced leaf size (Xiao et al., 2006; Olimpieri et al., 2011; Shohat et al., 2021). The conserved semi-dwarf phenotype conferred by GA20ox loss-of-function mutations across plant species demonstrated the critical role of GA homeostasis in height determination, establishing a mechanistic foundation for optimizing plant architecture through targeted editing of Green Revolution-related genes to enhance crop suitability in VF.

The Green Revolution was not the only historical event that revolutionized agricultural production through crop breeding. In tomato, two homologous genes, *SELF-PRUNING* (*SP*) and *SELF-PRUNING 5G* (*SP5G*), have played equally revolutionary roles in the global expansion and large-scale industrialization

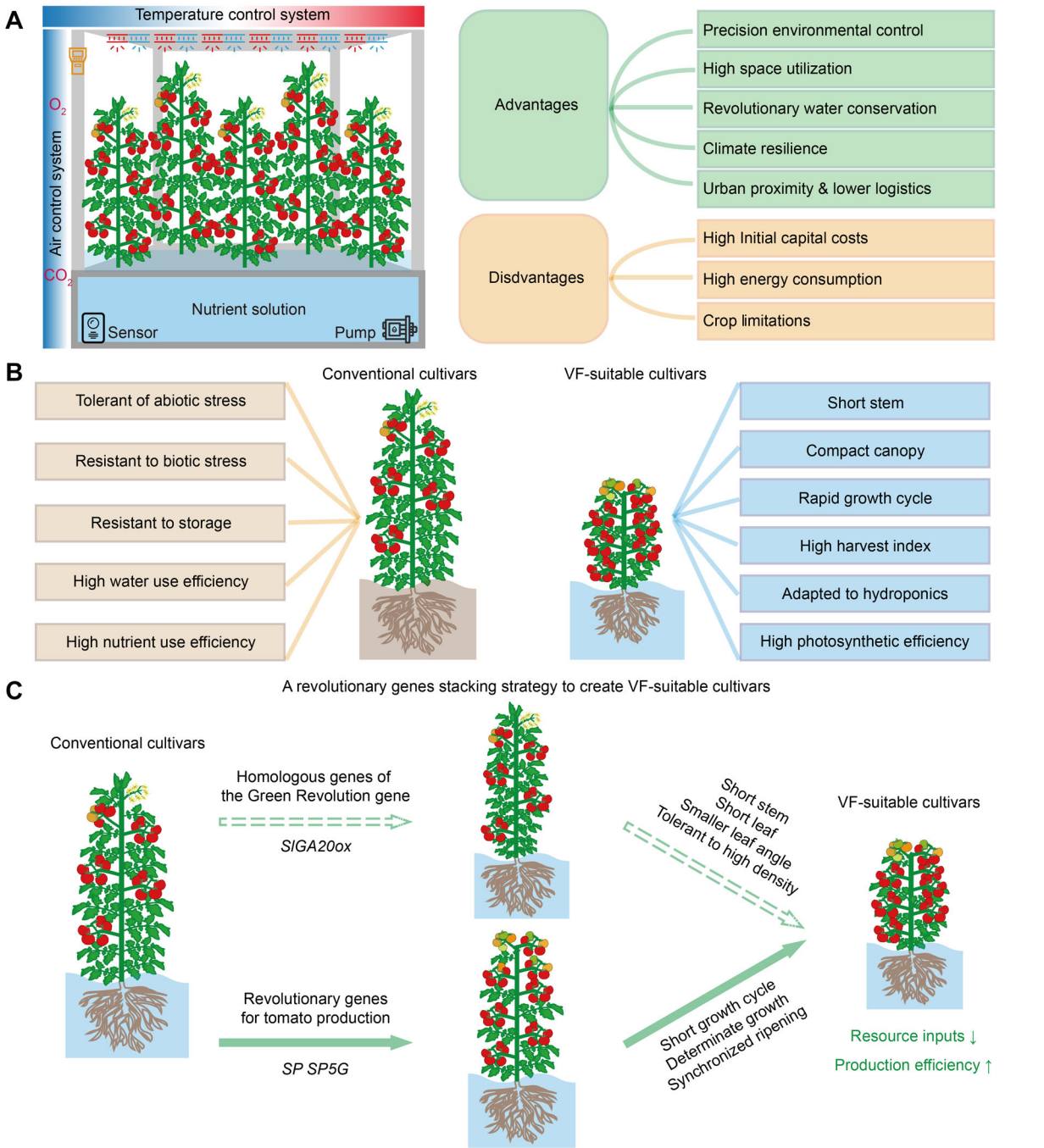

Figure 1. A strategy for stacking revolutionary genes to create vertical farming (VF)-suitable cultivars based on the characteristics of vertical farming

(A) Structure diagram and characteristics of VF. **(B)** Ideal traits for conventional cultivars and VF-suitable cultivars. **(C)** Diagram of stacking revolutionary genes to create VF-suitable cultivars.

of tomato production. The *SP* gene encodes anti-florigen, which regulates determinate growth by balancing the florigen–anti-florigen relationship (Yeager, 1927; Pnueli et al., 1998). The discovery of the *sp* variant in the 1920s enabled determinate growth, which facilitated faster cycles, higher planting densities, and mechanical harvesting, thereby enhancing efficiency and reducing labor costs for large-scale open-field production (Yeager, 1927; Eshed and Lippman, 2019). The *SP5G* primarily functions to inhibit flowering in tomato and plays a role in photoperiod regulation. The *sp5g* mutant demonstrated decreased sensitivity to day length and exhibited significantly earlier flowering (Soyk et al., 2017; Cao et al., 2018). The *sp sp5g* double mutant displayed earlier flowering, synchronized fruit ripening, and more compact plant architecture in the field (Soyk et al., 2017). Together, the *sp sp5g* variants increased yield, efficiency, and the geographical range of tomato

production, revolutionizing the agricultural landscape and enabling large-scale tomato production worldwide.

Here, we aimed to develop tomato germplasm optimized for VF through gene editing. The "Ailsa Craig" (AC) tomato cultivar was selected as our target for improvement, as it is a traditional greenhouse cultivar prized for salad production, as well as its established status as a model system in tomato biotechnology research (Lou et al., 2025). To address the low production efficiency of traditional tomato cultivars in commercial vertical farms, we utilized genome editing to integrate the valuable and functionally validated genes from traditional agriculture, including the Green Revolution-related genes *GA20ox* and two anti-florigen genes, *SP* and *SP5G*, to optimize plant architecture and growth cycles (Figure 1C).

RESULTS

Mutation of the *SlGA20ox1* resulted in a promising VF-suitable plant architecture

We selected the rice Green Revolution homologous gene family *GA20ox* as a target as it had been demonstrated to play a crucial role in plant architecture (Sasaki, 2002). Based on data from a previous study (Pattison et al., 2015) and phylogenetic analysis, we identified eight homologous *SlGA20ox* genes in tomato (Figure S1A). According to the expression patterns of *SlGA20ox* genes (Figure S1B), *SlGA20ox1* is primarily expressed in leaves, shoot apical meristems, pollen, and early fruits, while *SlGA20ox2* is mainly expressed in shoot apical meristems, and *SlGA20ox3* is primarily expressed in fruits; the other members exhibited relatively weak expression levels. We selected *SlGA20ox1* and *SlGA20ox2* as targets for optimizing tomato plant architecture suitable for VF by employing CRISPR/Cas9-mediated gene editing within the AC background. The frameshift mutations in both alleles of *SlGA20ox1* and *SlGA20ox2* led to the loss of gene function (Figure 2A).

We first analyzed the mutants' phenotypes in a solar greenhouse. The primary shoot length of *slga20ox1* was reduced by 34%–43%, and both sympodial shoot length and internode length were significantly shortened. In contrast, the *slga20ox2* mutant showed no significant differences compared with the WT (Figures 2B–E, S1C). In addition to the stem, the leaf length of *slga20ox1* was shortened by 27%–40%, and the leaf angle decreased by 18%–19%, indicating that the canopy structure of *slga20ox1* was more compact. The leaf of *slga20ox2* showed a slight shortening, while the leaf angle remained unaffected (Figure 2F–I). Moreover, *slga20ox1* exhibited a deeper leaf color, with chlorophyll content increased by 22%–25% (Figure 2J). In terms of reproductive growth, there were no significant differences in flowering time, length of inflorescence, number of flowers per inflorescence, and fruit setting rate of the *slga20ox1* and *slga20ox2* mutants compared with the WT (Figure S1C–H). However, the number of fruit trusses produced by *slga20ox1* and *slga20ox2* was significantly higher than that of the WT at the same plant height (Figure 2K). It is worth noting that the harvest index of *slga20ox1* was significantly increased, and its total soluble solids content was also markedly higher than that of the WT (Figure 2L, M), despite a slight reduction in yield per plant and single fruit weight compared with the WT (Figure S1I–L). Collectively, by knocking out the homologous genes of the rice Green Revolution gene in tomato, we successfully developed a tomato mutant with a semi-dwarf height and a compact canopy, without any obvious reproductive development defects; this has the potential for dense planting and holds promise for meeting the plant architecture demands in VF with limited space.

The *slga20ox1* mutant exhibited improved production efficiency in a commercial vertical farm

Next, we investigated the traits of the *slga20ox1* and *slga20ox2* mutants in a commercial vertical farm with multi-layered, LED-equipped automated hydroponic growth systems (Figures 3A, S2A) to determine whether the *slga20ox* mutant possessed advantages in VF production. In terms of space utilization, *slga20ox1* exhibited a significantly reduced vertical height of fruit trusses, along with shortened primary shoot length, sympodial shoot length, internode length, leaf length, and canopy width compared with the WT (Figures 3B–D), allowing for a higher number of fruit trusses at the same plant height and more red fruits per plant, leading to a 75% less space occupation of ripe fruits, while the *slga20ox2* showed a slight decrease in plant height and leaf length (Figures 3E–H, S3C, D). Additionally, we observed that the chlorophyll content in leaves of the *slga20ox1* and *slga20ox2* mutants was significantly higher than that in the WT (Figure S3E), suggesting that these mutants may exhibit increased photosynthetic efficiency or a delay in leaf senescence. Consistent with the results from the solar greenhouse, the flowering time and fruit setting rate of the *slga20ox1* and *slga20ox2* mutants were similar to those of WT (Figure S3F–H). However, the fruit ripening time of the *slga20ox1* mutant occurs approximately 2 days earlier than that of the WT, resulting in the number of red fruits significantly increased within the same growth period (Figure 3I, J), indicating that the *slga20ox1* has a faster harvesting cycle.

To accurately assess effective yield in VF, we divided per-plant above-ground biomass into effective yield (the fresh weight of ripe fruits) and extra biomass (the fresh weight of stems, leaves, and unripe fruits). The extra biomass consumes a portion of the lighting power and nutrients, and wastes additional space and labor for management. We calculated the ratio of effective yield to the total above-ground biomass of the above-ground part as the effective harvest index. The total biomass of *slga20ox1* per plant decreased by 16.6% (Figure S3I) and the extra biomass decreased by 42.2%, with a significant increase in fruit number, resulting in a 39.8% increase in effective yield and a 70.9% increase in effective harvest index, while *slga20ox2* showed a

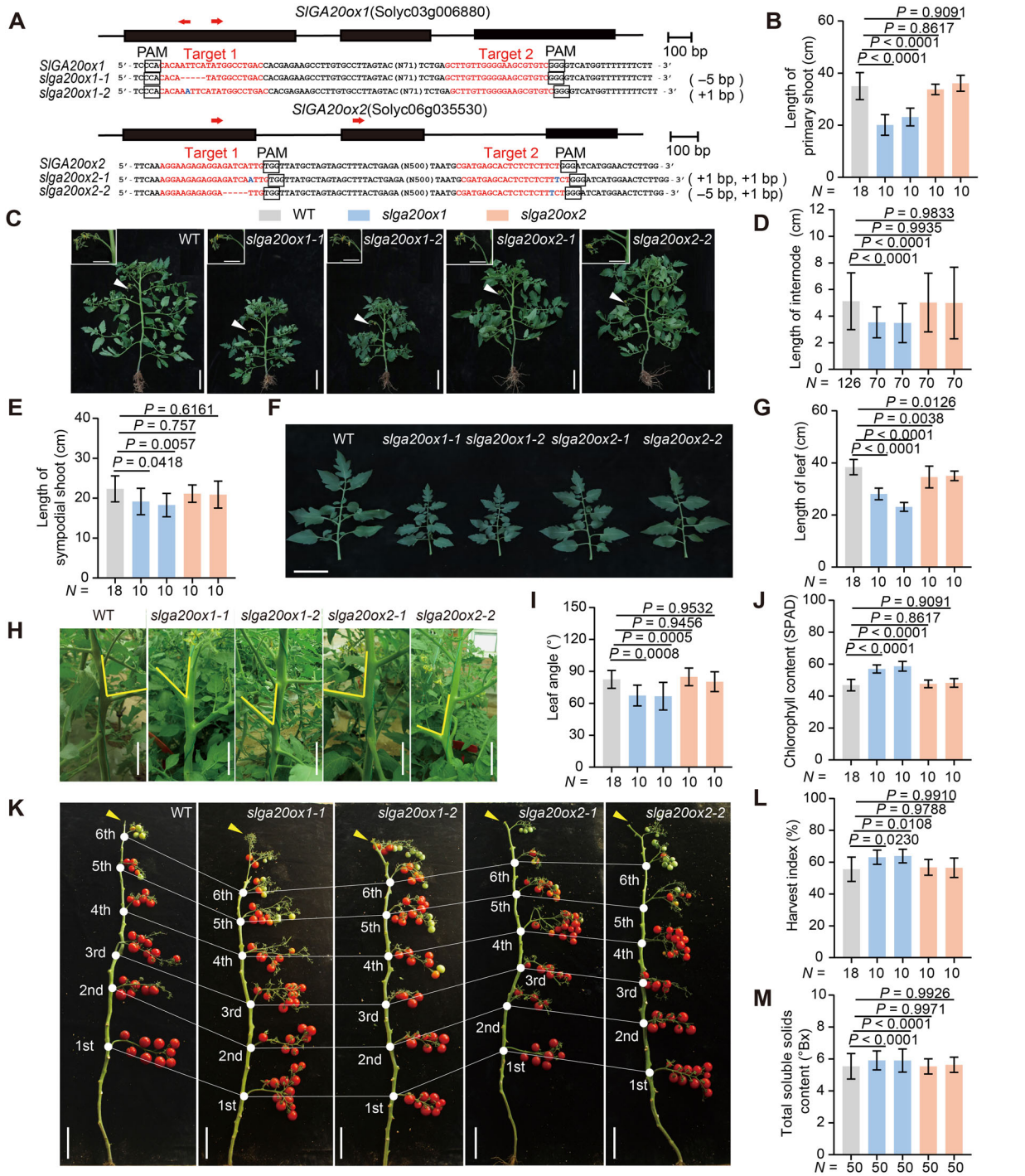

Figure 2. Mutations of Green Revolution homologous genes led to the semi-dwarfing of tomato

(A) The target design for CRISPR/Cas9 and the verified null mutation alleles of *SlGA20ox1* and *SlGA20ox2*. PAM, protospacer adjacent motif. **(B–E)** Representative images and quantitative data showing the length of the primary shoot **(B)**, internodes **(D)** and the sympodial shoot **(E)** The white arrowheads in **(C)** indicate the first inflorescence. **(F–J)** Representative images and quantitative data showing length of leaves **(F, G)**, leaf angle **(H, I)** and chlorophyll content **(J)**. The leaf angle is shown as a yellow angle in **(H)**. **(K)** Representative images showing the fruit truss height. The height of the first truss represents the primary shoot and the stem between the subsequent fruit trusses represents the sympodial shoot. The yellow arrowheads indicate the height to be pruned, apical portions above which have been manually removed. The white dots in **(K)** indicate the fruit truss position on the shoot. The sequence number indicates the sequence of fruit truss. **(L, M)** Quantitative data of harvest index and total soluble solids content. *N*, number of individual plants in **(B)**, **(E)**, **(G)**, **(I)**, **(J)**, and **(L)**, number of internodes in **(D)** and number of fruits in **(M)**. Scale bars, 5 cm in **(C)** and **(H)** and 10 cm in **(F)** and **(K)**. The *P*-values were determined using one-way analysis of variance (ANOVA) and Dunnet test for multiple comparisons. All data are shown in means ± *SD*.

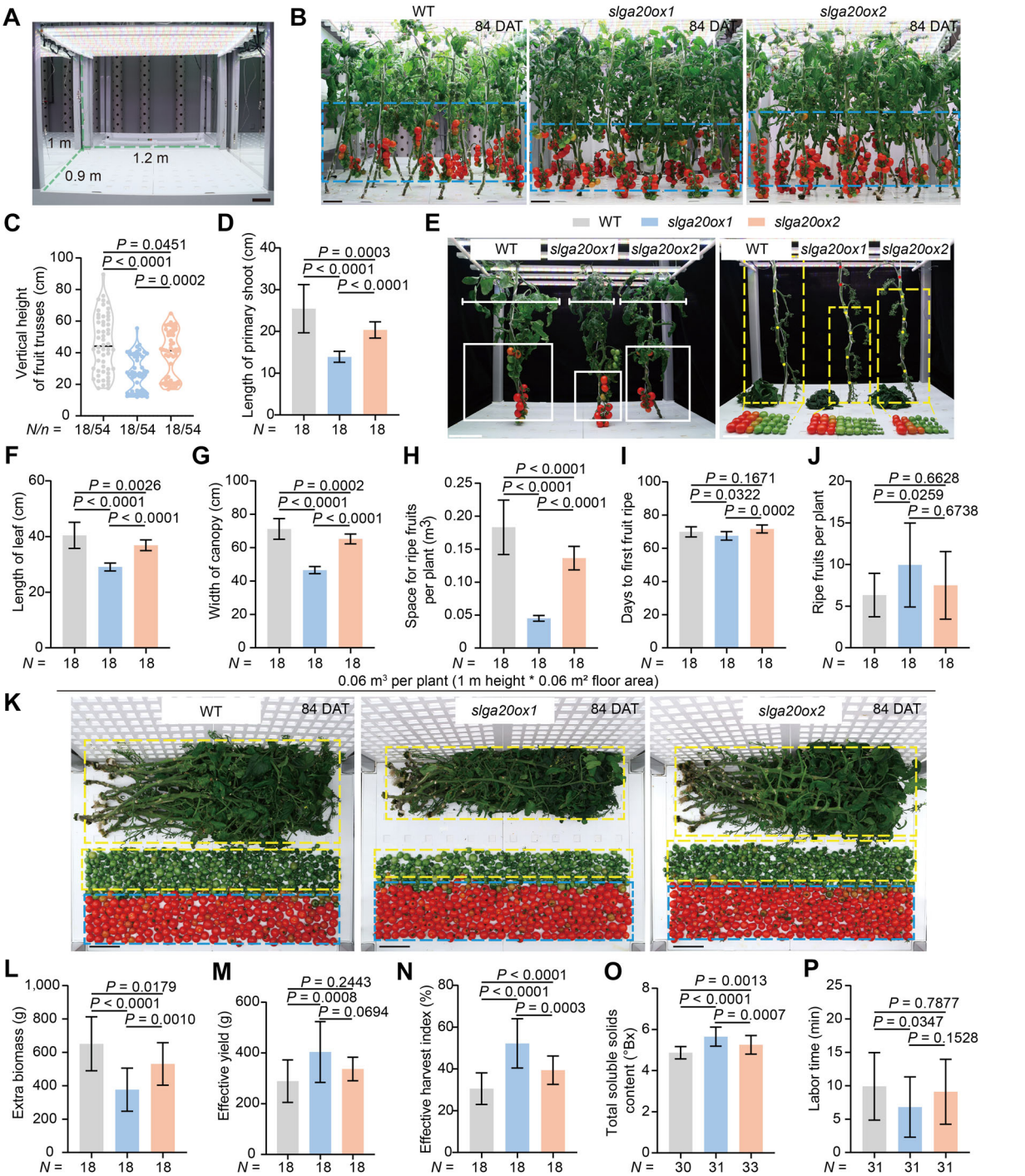

Figure 3. Semi-dwarf tomato enhanced the production efficiency in vertical farming (VF)

(A) Image of a single layer hydroponic module of VF. **(B, C)** Representative images and quantitative data show the vertical space for ripe fruits in VF. Blue dashed box in **(B)** indicates the space for the ripe fruit trusses per layer. DAT, days after transplanting. **(D–H)** Representative phenotypes of wild-type (WT), *slga20ox1* and *slga20ox2* and related quantitative data of primary shoot height **(D)**, length of leaves **(F)**, the width of the canopy **(G)** and space for ripe fruits per plant **(H)**. The white line in **(E)** indicates the canopy width. The white box in **(E)** indicates the space for the ripe fruit trusses per plant. The yellow dashed boxes in **(E)** indicate the space for the first four fruit trusses per plant. The yellow dots and red dots in **(E)** indicate the fruit truss position on the shoot. **(I–P)** Representative phenotypes of WT, *slga20ox1* and *slga20ox2* and related quantitative data of DAT to first ripe fruit **(I)**, ripe fruits per plant **(J)**, extra biomass **(L)**, effective yield **(M)**, effective harvest index **(N)**, total soluble solids content **(O)** and time of manual management per layer each time **(P)**. The blue dashed boxes in **(K)** indicates the effective yield (ripe fruits). The yellow dashed boxes in **(K)** indicate the extra biomass (stems, leaves and unripe fruits). *N*, number of individual plants in **(C, D)**, **(F–J)** and **(L–N)**, number of fruits in **(O)** and number of manual management times in **(P)**. *n*, number of fruit trusses. Scale bars, 10 cm. The *P*-values were determined using one-way ANOVA and Tukey test for multiple comparisons. All data are shown in means ± *SD*.

16.5% increase in effective yield and 28.9% increase in effective harvest index (Figures 3K–N, S3J–L). This suggests that by modifying *SlGA20ox1* and *SlGA20ox2*, a portion of the lighting energy and nutrients that would have been used to generate extra biomass was redirected to fruit effective yield. Despite a slight decrease in single fruit weight (Figure S3M–O), the total soluble solids content of the fruits from both *slga20ox1* and *slga20ox2* still significantly increased (Figure 3O).

Although tomato production is highly mechanized in open fields, actual production in greenhouse and VF still requires complex manual management tasks such as pruning leaves and removing lateral branches. The optimized tomato plant architecture may facilitate manual management; therefore, we timed each manual operation (including leaf pruning and lateral branch removal) for each genotype. Our analysis demonstrated that the *slga20ox1* mutation achieved a 31.3% reduction in the average labor time required per task compared with the WT (Figure 3P). These findings indicated that modification of *SlGA20ox* genes optimized tomato production efficiency in a commercial vertical farm by reducing space occupation, shortening harvest timelines, and decreasing labor inputs.

The *slga20ox1* mutant enhanced production efficiency under high-density planting

In order to fully utilize environmental resources, crops need to be stacked not only in vertical space, but also planted at high density in each layer of the hydroponic module (Kozai and Niu, 2016). To evaluate the yield of the *slga20ox1* and *slga20ox2* mutants through dense planting in a commercial vertical farm, we increased the planting density to 300%, from 16 plants per layer to 48 plants per layer within the same module volume (Figures 4A, S2B).

Under high density, the primary shoot length, sympodial shoot length, and internode length of *slga20ox1* and *slga20ox2* were significantly shortened, and the vertical height of fruit trusses, canopy width and leaf length were decreased significantly but with high chlorophyll content in leaves (Figures 4A–D, S4A–E). Flowering and fruit ripening times of *slga20ox1* were both significantly early (Figures 4E, S4F, G). Moreover, the fruit setting rate and number of fruits of *slga20ox1* were significantly higher than those of *slga20ox2* and the WT (Figure S4H, I). Under 300% density planting conditions, the effective yield of *slga20ox1* increased by 69%, and the effective harvest index increased by 101%, while *slga20ox2* also had a 26.4% increase in effective yield and a 21% increase in effective harvest index (Figures 4F–H, S4J, K). Furthermore, the total soluble solids content of *slga20ox1* remained significantly higher than that of the WT (Figure 4I). The high-density planting significantly increased the labor time required to ensure healthy plant growth. However, *slga20ox1* achieved a 29.5% reduction in labor time (Figures 3P, 4J), thus saving substantial labor under high-density planting conditions. These results indicated that *slga20ox1* could significantly enhance tomato effective yield and harvest index under 300% density planting conditions. Although the *slga20ox1* mutant exhibited a 47% decrease in per-plant effective yield compared with low-density planting, the total effective yield per layer increased by 42% due to the larger number of plants.

High-density planting of *slga20ox1* improved production efficiency with less space occupation and lower lighting power consumption

A typical feature of VF is the allowance for multi-layer stacking of crop production modules to enhance space utilization efficiency. We tested whether it was possible to reduce the height of each layer to improve space utilization efficiency and thereby enhance production efficiency. We used hydroponic modules with a 0.4 m height, the size of which is widely used for producing leafy vegetables like lettuce. In terms of lighting, we reduced the number of LEDs per layer from 15 to six, achieving a 60% reduction in lighting power consumption. (Figures 4K, S2C, D). After estimation, we adjusted the planting number to 30 plants per layer (Figure S2E), the space occupation of each tomato plant was only 0.0144 m^3 with a 0.4 m height. This planting density reaches 416% of the commercial vertical farm (Figures 3, S2A).

As expected, *slga20ox1* still demonstrated a higher vertical space utilization efficiency, more fruit, and faster maturity, with a 38% higher effective yield and 31% higher effective harvest index than those of WT. Additionally, it reduced the labor time per management task by 28.8% (Figures 4K–R, S5), while the weak phenotype of *slga20ox2* showed no practical effects under such high spatial density. Hence, moderate dense planting of *slga20ox1* could effectively enhance its space utilization efficiency in VF. These data demonstrated that high-density planting of *slga20ox1* in a commercial vertical farm enhanced production efficiency while reducing space occupation and energy costs.

Combining revolutionary genes to create a VF-suitable cultivar

The improved production efficiency of the *slga20ox* mutants in commercial VF conditions prompted us to investigate whether two other revolutionary genes, *SP* and *SP5G*, could maintain optimized plant architecture and accelerated harvest cycle in VF conditions. To test this, we generated the *sp sp5g* double mutant in the AC background using CRISPR/Cas9 technology (Figure 5A). The *sp sp5g* double mutant exhibited early flowering and determinate growth phenotypes (Figure S6), which were critical for VF-suitable cultivars. To integrate these improvements with GA-mediated yield enhancement, we crossed the *slga20ox1* and *slga20ox2* mutants with the *sp sp5g* double mutant, respectively, resulting in *sp sp5g slga20ox1* and *sp sp5g slga20ox2*. Next, we conducted a phenotype analysis of these mutants in the same vertical farm mentioned above (Figure 3A). In terms of space utilization efficiency, the vertical height of fruit trusses of *sp sp5g slga20ox1* was

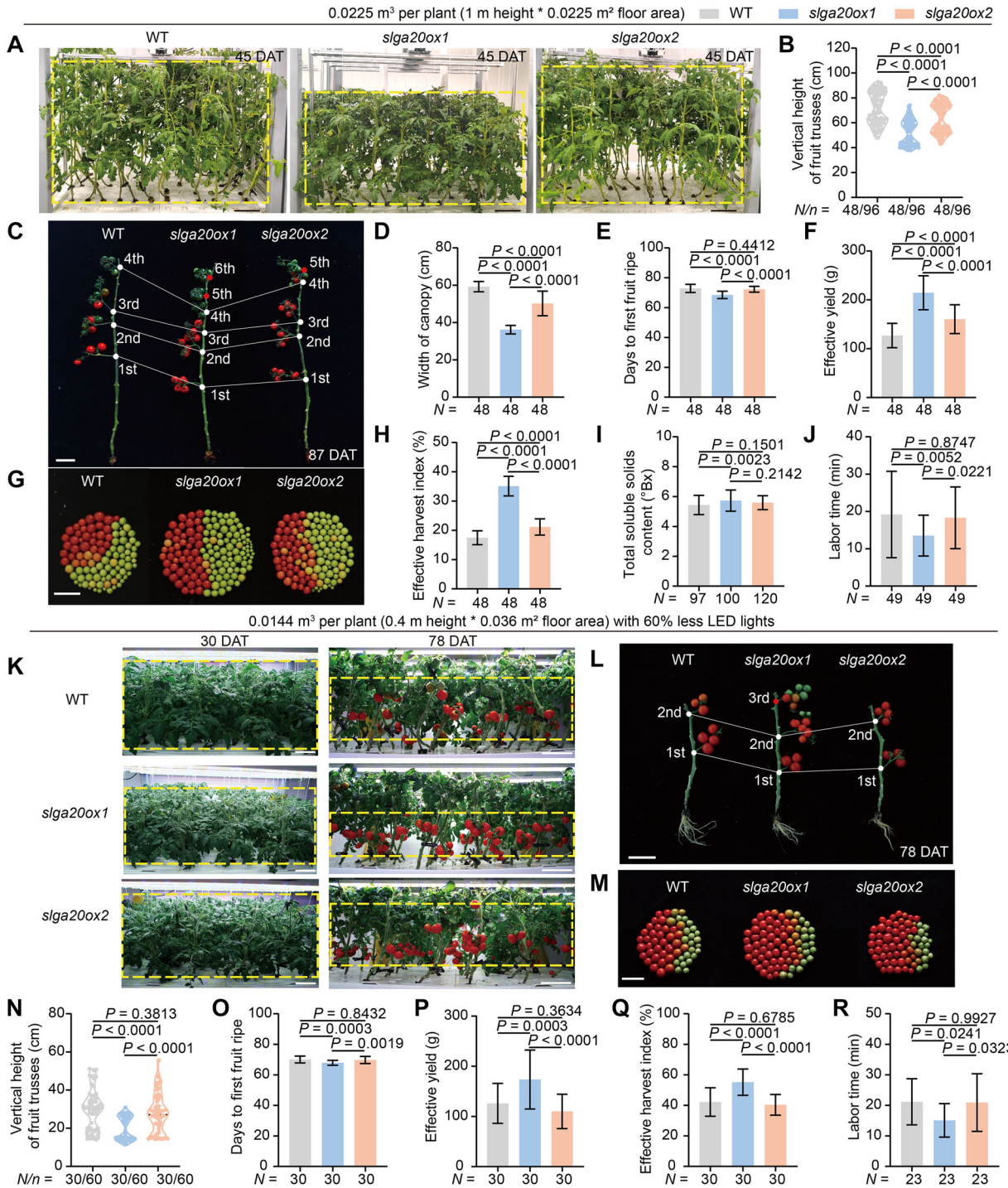

Figure 4. High-density planting of *slga20ox1* improved production efficiency with less space occupation and lower lighting power consumption
(A) Representative images showing the vertical space for plants under 0.0255 m^3 space on average in vertical farming (VF). The yellow dashed boxes indicate the space for plants. **(B)** Quantitative data of the vertical height of each fruit truss. **(C–J)** Representative phenotypes of wild-type (WT), *slga20ox1* and *slga20ox2* under 0.0255 m^3 space on average and related quantitative data of width of canopy **(D)**, days after transplanting (DAT) to first ripe fruit **(E)**, effective yield **(F)**, effective harvest index **(H)**, total soluble solids content **(I)**, and manual management per layer each time **(J)**. White dots in **(C)** indicate the fruit trusses position on the shoot. Sequence number indicates the sequence of fruit truss. **(K)** Representative images showing the vertical space for plants and ripe fruits under 0.0144 m^3 space on average in VF. Yellow dashed boxes indicate the space for plants at 30 DAT and the space for ripe fruits at 78 DAT. **(L–R)** Representative phenotypes of WT, *slga20ox1* and *slga20ox2* under 0.0144 m^3 space on average and related quantitative data of the vertical height of each fruit truss **(N)**, days after transplanting to first ripe fruit **(O)**, effective yield **(P)**, effective harvest index **(Q)** and manual management per layer each time **(R)**. White dots in **(L)** indicates the fruit trusses position on the shoot. Sequence number indicates the sequence of fruit truss. *N*, number of individual plants in **(B)**, **(D–F)**, **(H)**, **(N–Q)**, number of fruits in **(I)** and number of manual management times in **(J)** and **(R)**. *n*, number of fruit trusses. Scale bars, 10 cm. The *P*-values were determined using one-way ANOVA and Tukey test for multiple comparisons. All data are shown in means ± *SD*.

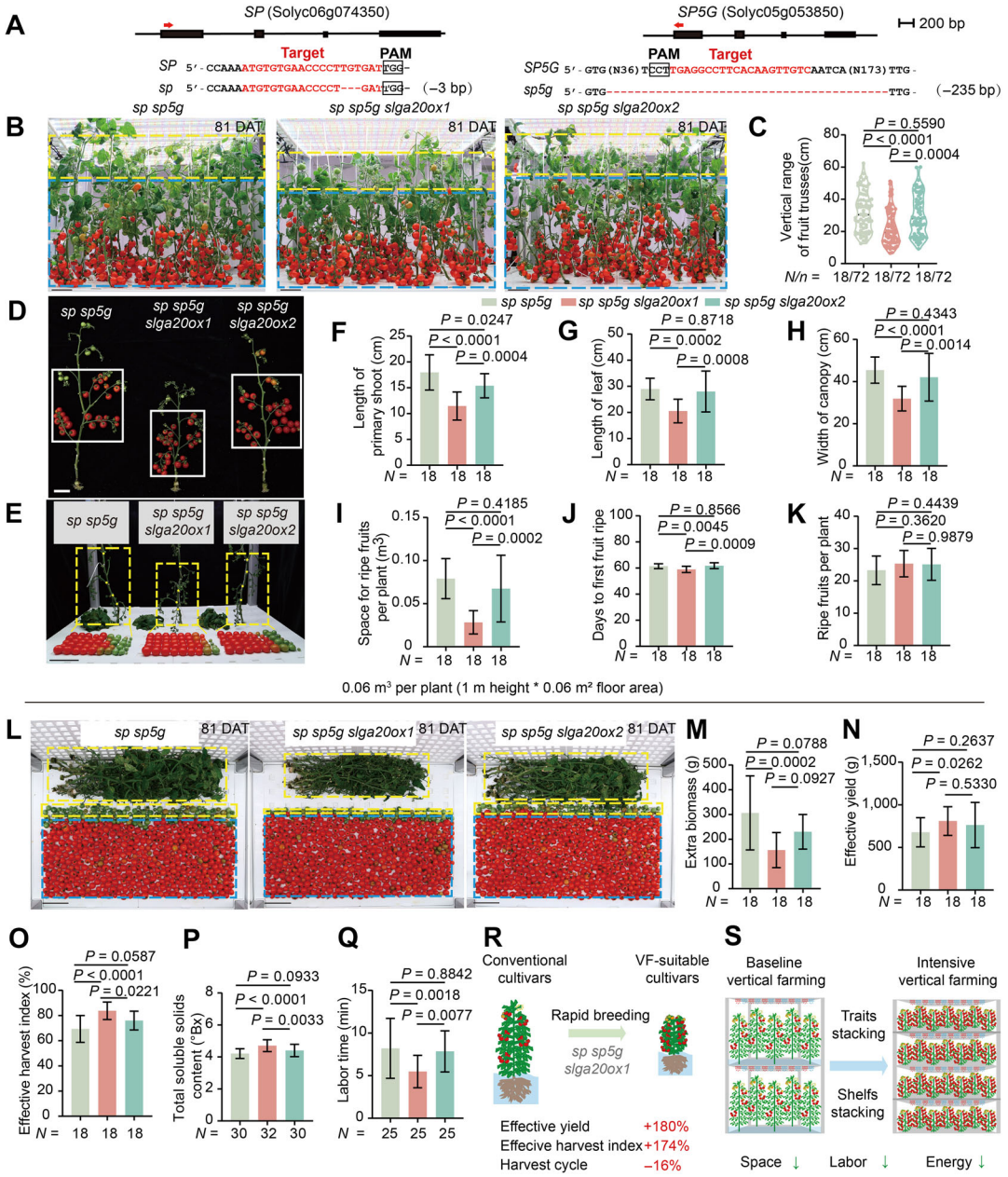

Figure 5. Combination of revolutionary genes to create a vertical farming (VF)-suitable cultivar

(A) The CRISPR/Cas9 targets and verified null mutation alleles of *SP* and *SP5G*. **(B)** Representative images showing the vertical space for ripe fruits and extra biomass in VF. Blue dashed boxes indicate the space for ripe fruits. Yellow dashed boxes indicate the space for extra biomass above ripe fruits. **(C)** Quantitative data of the vertical height of each fruit truss. **(D–K)** Representative phenotypes of *sp sp5g*, *sp sp5g slga20ox1*, and *sp sp5g slga20ox2* and related quantitative data of primary shoot height **(F)**, length of leaves **(G)**, width of canopy **(H)**, space for ripe fruits per plant **(I)**, days after transplanting (DAT) to first ripe fruit **(J)** and ripe fruits per plant **(K)**. White boxes in **(D)** indicate the space for the ripe fruit trusses per plant. The yellow dashed boxes in **(E)** indicate the space for ripe fruits per plant. The yellow dots in **(E)** indicate the fruit truss position on the shoot. **(L–Q)** Representative phenotypes of *sp sp5g*, *sp sp5g slga20ox1*, and *sp sp5g slga20ox2* and related quantitative data of extra biomass **(M)**, effective yield **(N)** and effective harvest index **(O)**. Blue dashed boxes in **(L)** indicate the effective yield (ripe fruits). The yellow dashed boxes in **(L)** indicate the extra biomass (stems, leaves, and unripe fruits). **(P, Q)** Quantitative data of total soluble solids content **(P)** and time of manual management per layer each time **(Q)**. **(R)** Diagram of one step to create tailored cultivars for VF. The ratios were calculated by comparing *sp sp5g slga20ox1* to wild-type (WT) under the same conditions in VF. **(S)** Diagram of how VF-suitable cultivars benefit the equipment and cultivation optimization in VF production. The ratio of space represents the height of the module as 60% reduced compared with a commercial module in VF. The ratio of lighting energy represents the lighting energy as 60% less than a commercial module in VF. The ratios of harvest cycle and labor were calculated by comparing *sp sp5g slga20ox1* to WT under the same commercial vertical farm. *N*, number of individual plants in **(C)**, **(F–K)**, **(M–O)**, the number of fruits in **(P)** and the number of manual management times in **(Q)**. *n*, number of fruit trusses. Scale bars, 10 cm. The *P*-values were determined using one-way ANOVA and Tukey test for multiple comparisons. All data are shown in means ± *SD*.

reduced by 30.8% compared with the *sp sp5g* mutant (Figure 5B, C), accompanied by significant reductions in primary shoot length, sympodial shoot length, internode length, canopy width, and leaf length (Figures 5D–H, S7A, B). Consequently, the *sp sp5g slga20ox1* mutant reduced ripe fruit space occupancy by 64% compared with *sp sp5g* and by 85% compared with WT (Figure 5H; Table S1). Additionally, the *sp sp5g slga20ox1* mutant had a significant increase in leaf chlorophyll content (Figure S7C). Notably, the *sp sp5g slga20ox1* triple mutant showed identical flowering synchrony to that of the *sp sp5g* (Figure S7D–F). In terms of fruit ripening, the *sp sp5g slga20ox1* triple mutant was approximately 2 days earlier than that of *sp sp5g* and about 11 days earlier than WT (Figure 5J–K; Table S1). However, despite a 14.3% reduction in primary shoot length, other traits of *sp sp5g slga20ox2* were not statistically different from those of *sp sp5g* (Figure 5B–K).

With regard to production efficiency, compared with the *sp sp5g* mutant, the *sp sp5g slga20ox1* triple mutant displayed a 19.4% increase in effective yield, a 20.8% increase in effective harvest index and a 49.1% reduction in extra biomass, along with a 33.2% reduction in labor time per management task. In addition, the total soluble solids content of *sp sp5g slga20ox1* was significantly higher than *sp sp5g*. In contrast, *sp sp5g slga20ox2* exhibited a slight improvement, but this was not statistically significant (Figures 5L–Q, S7H, I). Thus, the *sp sp5g slga20ox1* triple mutant effectively gathered the advantages of traits from its respective mutants, making it suitable for the rapid breeding of VF-suitable cultivars.

In summary, using the AC as the tomato model, which has lower adaptability in VF, we stacked valuable and functionally validated genes from traditional agriculture to rapidly develop a VF-suitable cultivar that enhanced space utilization efficiency, accelerated fruit ripening, and reduced labor costs in VF. Under the same commercial VF condition, this improved cultivar could reduce space occupation by 85%, shorten the harvest cycle by 16%, and achieve a 180% increase in effective yield and a 174% increase in effective harvest index compared with WT (Figure 5R; Table S1). Moreover, the modifications to shoot length and canopy structure by *slga20ox1* endowed tomato with a tolerance to high-density planting, allowing more efficient utilization of spatial and environmental resources that enabled vertical stacking of more cultivation layers, significantly increasing the effective yield and production efficiency with the same or fewer resources in commercial vertical farms (Figure 5S).

DISCUSSION

The development of VF can be traced back to the 20th century, but its practical implementation commenced in the early 21st century. Against the backdrop of accelerating urbanization, escalating climate change, and growing food security concerns, VF has progressively emerged as a crucial supplementary form within modern agricultural systems (Zhu and Marcelis, 2023). This evolution from theoretical concept to industrial application epitomizes humanity's ingenuity in overcoming resource constraints through technological innovation. Despite current challenges including high operational costs, substantial energy consumption, and limited crop adaptability (Kozai and Niu, 2016; van Delden et al., 2021), VF demonstrates irreplaceable value in safeguarding urban food security, enhancing resource efficiency, and improving climate resilience.

To address these bottlenecks, beyond technological innovations for energy and cost reduction, the paramount solution lies in developing crop cultivars that are specifically adapted to the unique growing conditions of vertical farms, thereby substantially boosting agricultural production efficiency. VF systems require crops with dwarf stature, compact architecture, rapid growth cycle and high photosynthetic efficiency (Kwon et al., 2020; SharathKumar et al., 2020). Consequently, the strategic development of genetically modified VF-adapted cultivars through targeted genetic engineering emerges as a pivotal approach to overcoming crop limitations. This methodology aligns with the seminal success of the Green Revolution (Hedden, 2003), where the introduction of dwarfing traits effectively resolved issues of lodging and low yields in high-fertilizer cultivation environments.

In this study, we proposed a paradigm shift from passive environmental adaptation to active genetic gain engineering by bridging Green Revolution genetics with VF requirements. As shown in Figure 1, this paradigm leverages scenario-specific gene–environment interplay to achieve high-yield amplification in controlled agricultural systems. Knockout of *SlGA20ox1* and *SlGA20ox2* in tomato resulted in a semi-dwarf plant phenotype with shortened stems and compact canopies, yet also reduced fruit yield due to smaller fruit size under solar greenhouse conditions (Figures 2, S1). This architectural modification paralleled the semi-dwarf stature and decreased single-plant yield observed in the rice Green Revolution mutant *sd1* (Su et al., 2021). Crucially, cereal crops like semi-dwarf rice and wheat achieved significant yield gains per unit area through high-density planting and enhanced lodging resistance (Hedden, 2003). The *slga20ox1* mutant exhibited a pronounced semi-dwarf phenotype both in soil-cultivated greenhouses and in vertical farms, while the *slga20ox2* mutant showed a weaker phenotype (Figures 2, 3). Studies have shown that the spatiotemporal expression patterns (temporal and spatial specificity) of genes in plants critically influence their functions by determining the activity scope and biological effects. We propose that the phenotypic differences between *slga20ox1* and *slga20ox2* mutants may be mainly due to the different expression patterns of *SlGA20ox1* and *SlGA20ox2* genes during tomato development. *SlGA20ox1* shows high expression levels in leaves during the vegetative growth stage, which probably has a

great impact on plant architecture. In contrast, *SlGA20ox2* exhibited low expression in vegetative tissues but was predominantly expressed in the sympodial inflorescence meristem (SIM) and flower meristem (FM), suggesting a limited role in shoot morphology regulation (Table S1B). Consistent with these expression profiles, the *slga20ox1* mutant displayed a pronounced semi-dwarf phenotype, while the *slga20ox2* mutant exhibited a weaker phenotype. These findings indicated that the spatiotemporal expression patterns of *GA20ox* genes in plants could serve as critical criteria for selecting optimal genetic targets to optimize plant architecture in VF. By implementing analogous high-density planting in VF, we substantially augmented the yield per unit space in *slga20ox*1 mutants (Figures 3, 4). Critically, the *slga20ox1* mutant when cultivated with only six LEDs achieved a yield comparable with WT with 15 LEDs, suggesting that the light energy use efficiency of *slga20ox1* was increased (Figures 3K, M, 4K, P), and suggesting its higher light energy use efficiency. The enhanced light energy use efficiency observed in *slga20ox1* mutants may be attributed to their compact plant architecture. This compact canopy improves light distribution and reduces light competition to enhance the efficiency of light capture by crops (Tian et al., 2024), thereby enabling high-density planting to improve yield, which is consistent with the yield increase seen in compact crops during the Green Revolution (Hedden, 2003). These results demonstrated that VF's optimized vertical spatial utilization amplifies the yield-boosting effects of Green Revolution genes, effectively transitioning their agricultural value from conventional planar systems to advanced three-dimensional cultivation systems. Furthermore, the water deficiency tolerance of *slga20ox1* and *slga20ox2* (Shohat et al., 2021) is potentially beneficial for optimizing automated irrigation management in VF and further improving water use efficiency. These results indicated that genes constrained by phenotypic limitations in traditional agriculture could regain adaptive advantages in VF, enabling scenario-specific reactivation of genetic resources.

Significantly, beyond the canonical Green Revolution genes, critical signaling networks regulating plant architecture, developmental phases, and photosynthetic efficiency all present viable genetic targets for VF-suitable cultivar improvement. Notably, certain genetic modules that were evolutionarily disfavored in conventional field environments due to their association with undesirable phenotypes may find renewed utility in VF systems with precisely controlled spectral conditions. The brassinosteroid (BR) signaling pathway serves as a regulator of plant architecture through its dual control of cell elongation/division and organogenesis (Kim and Russinova, 2020). Whereas BR-deficient mutants (e.g., Arabidopsis *det2*, rice *brd1*) exhibit extreme dwarfism and are compact, which render them agriculturally nonviable in conventional field settings (Chory et al., 1991; Clouse et al., 1996; Yamamuro et al., 2000; Mori et al., 2002). Markedly, these "disadvantageous" phenotypes become strategic advantages in commercial vertical farms, where the spatially constrained environments of multi-layer hydroponic platforms synergize with the mutants' reduced vertical growth to optimize light distribution and space utilization efficiency. This paradigm effectively decouples the historical trade-off between architectural compactness and photosynthetic productivity observed in horizontal farming systems.

In addition, the full-spectrum programmable LEDs in VF enable novel evolutionary scenarios, driving innovations in light-related genetic adaptations. By genetically manipulating genes associated with light pathways, we can significantly enhance the light utilization efficiency of plants in VF. By engineering the key photosynthesis genes (like RuBisCO), photoperiod response genes (like *PHYB* and *HY5*) can optimize plant growth under varying light conditions (Jansson, 1994; Morita et al., 2015; Cheng et al., 2021; Suganami et al., 2021). Additionally, altering leaf morphology and structure (Liu et al., 2021) and enhancing the synthesis of photosynthetic pigments can improve light capture capability (Wang and Grimm, 2021). The combined application of these genetic manipulation strategies will significantly enhance the light utilization efficiency of plants, ultimately improving crop yield and quality. In the future, robotics will serve as a core driver for achieving scalability and intelligence in VF (Daum, 2021). Establishing robotic vertical farms demands groundbreaking innovations at the intersection of biology and mechanical engineering. The synergistic integration of biosystems and automation is forging intelligent agricultural production systems, elevating VF to an era of industrial-grade precision cultivation.

Overall, improving the production efficiency of VF mainly involves two approaches: adopting new industrial technologies to enhance equipment performance, and using advanced biotechnology to improve the genetic gain of crops tailored for vertical systems. Our work showcased how to utilize agricultural practice-validated genes to rapidly improve crop genetic gain and production efficiency in VF.

MATERIALS AND METHODS

Plant materials and growth conditions

Tomato (*Solanum lycopersicum*) cultivar AC was used in this study. For plants in a solar greenhouse, seeds were directly sown in soil in 72-cell plastic flat trays. Seedlings with four to five true leaves were transplanted to soil under natural light and temperature.

The yield trials in VF were conducted in a commercial vertical farm with automated hydroponic growth systems. The hydroponic modules (RADIX; SANANBIO, Fujian, China) were multi-layered and the height of each layer could be flexibly adjusted between 0.2–1.5 m through modular assembly. In terms of lighting, each layer of the hydroponic module was equipped with 15 detachable LED tubes (skylark, ZK3-TB18-VE02/A; SANANBIO, Fujian, China) in

commercial production. The vertical height and LED number of each layer could be flexibly controlled by assembling modules of different heights and removing or installing the LEDs. The photosynthetic photon flux (PPF) was 38 μmol s^{-1} per LED lamp tube. The photosynthetic photon flux density (PPFD) to the middle height of the module was measured to 200 μmol m^{-2} s^{-1} on the 1 m high commercial module with 15 LEDs. On the 0.4 m high module with six LEDs, the PPFD to the middle height of the module was measured to 110 μmol m^{-2} s^{-1}. For plants cultivated in the hydroponic vertical farm, seeds germinated on moist filter paper were transferred into sponge substrates within plastic trays. The sponge substrates were kept moist by daily replenishment with water. After cotyledon expansion, the water was replaced with the hydroponic nutrient solution. Seedlings with three to four true leaves were transplanted into hydroponic modules. Growth conditions were maintained at 26°C (day)/22°C (night) under a 16-h light/8-h dark photoperiod with 40%–60% relative humidity. The structural dimensions of the hydroponic module are illustrated in Figures 3A, S2D.

An automated nutrient solution circulation system was used in the hydroponic module. The prepared nutrient solution was stored in a water tank and delivered to the cultivation layers via an automated water pump. The solution flowed through all cultivation layers by gravity and subsequently returned to the water tank. The nutrient solution was replenished or replaced every 1–2 weeks. The pH of the hydroponic nutrient solution was 5.8 and the electrical conductivity (EC) was 0.5 dS/m for seedlings in the trays, 0.8–1.2 dS/m from transplantation to the flowering stage, and 1.5–2.0 dS/m from flowering to harvest.

Phylogenetic analysis

A phylogenetic tree was constructed using the maximum likelihood (ML) method in MEGA X. The bootstrap consensus tree was inferred from 1,000 bootstrap replicates.

Guide RNA design and CRISPR/Cas9 constructs

To generate *slga20ox1* or *slga20ox2* single mutant and *sp sp5g* double mutant, gene-specific guide RNAs for targeting exons were designed using the online tool (http://cbi.hzau.edu.cn/cgi-bin/CRISPR). Guide RNAs for each gene were constructed using standard Golden Gate assembly, as described before (Brooks et al., 2014; Li et al., 2018).

Generation and genotyping of the transgenic plants

The constructs were transformed into plants by *Agrobacterium*-mediated transformation and tissue-culture protocols as described before (Li et al., 2018). Genomic DNA of first-generation (T0) transgenic plants was extracted using the cetyltrimethylammonium bromide (CTAB) method. CRISPR/Cas9 induced mutations; identified mutations in target genes were genotyped using the Ultra Taq PCR StarMix (ZA019-101S; GenStar, Beijing, China) and specific primers (Table S2), followed by Sanger sequencing validation.

Biomass and fruit yield evaluation

During manual management, lateral shoots and senescent leaves were removed. At harvest, the fresh weights of unripe fruits (at or before the breaker stage), ripe fruits (red-ripe stage), stems, and leaves were measured. The total biomass was calculated as the sum of the fresh weight of all tissues (above-ground) per plant. The extra biomass was defined as the sum of the fresh weight of unripe fruits, stems, and leaves. The total yield was calculated as the sum of the fresh weight of all fruits, while the effective yield was defined as the sum of the fresh weight of ripe fruits. The harvest index was calculated using the ratio of total yield and total biomass. The effective harvest index was calculated by the ratio of effective yield to total biomass. Single fruit weight was measured on a standard electronic scale. Fruit diameter was measured using standard vernier calipers.

Plant phenotyping and data collection

Transgene-free homozygous plants were used to obtain phenotypes in a greenhouse and a vertical farm. All phenotypes related to length, width and height were measured manually with a ruler or tape measure. The length of primary shoots and internodes was measured when most flowers had opened in the first inflorescence. The length of the sympodial shoot was measured when most flowers had opened in their inflorescence. The first leaf under the first inflorescence was used to measure the length of leaves and leaf angle. The width of the canopy was measured as the straight distance between the tips of the two leaves furthest apart. The space for ripe fruits per plant (S) was calculated from the height of the highest truss of ripe fruit (H) and the width of the canopy (W) by calculating the volume of the column for each plant. The calculation formula is $S = 3.14(W/2)^2 \times H$.

The leaves-to-flower transition was measured by counting the number of true leaves under the first inflorescence. The days to the first flower and first ripe fruit were observed and recorded every day. The fruit setting rate was calculated by the ratio of fruits and flowers in each inflorescence. Total soluble solids content was measured using a Brix meter PAL-1 (ATAGO, Tokyo, Japan).

Measurements of chlorophyll content

The first leaf under the first inflorescence was used to measure the chlorophyll content and photosynthetic activity. The chlorophyll content was measured using a handheld SPAD -502 (Konica Minolta, Tokyo, Japan).

Measurement of manual management labor time

Manual management included the removal of lateral shoots and pruning of leaves. The growth of plants in the hydroponic modules was monitored daily. When lateral shoots emerged from leaf axils, leaves overlapped severely, or bottom leaves exhibited senescence, manual management was performed. The labor time required for each manual management per genotype was recorded using a stopwatch.

Gene annotation and accession numbers

Gene sequences of *SlGA20ox1 and SlGA20ox2* were obtained from the Sol Genomics Network (SGN) database (https://solgenomics.net/). Amino acid sequences of GA20ox homologous proteins were obtained from Phytozome v13 (https://phytozome-next.jgi.doe.gov/) and NCBI (https://www.ncbi.nlm.nih.gov/). Genes and corresponding accession numbers are shown in Table S3. The expression atlas of *SlGA20ox* genes was from our laboratory's transcriptome data.

Statistical analyses

Statistical calculations were conducted using GraphPad Prism 8.0. The statistical information for each analysis is provided in the respective figure legends, including the statistical tests used and the exact value of sample size. Results are represented as mean ± standard deviation. The *P*-values are indicated above each bar graph.

Data availability statement

The data that support the findings of this study are available from the corresponding author upon reasonable request.

ACKNOWLEDGEMENTS

We thank Xiaoran Liu for assistance with the management of vertical farms. We thank Dr. Jing Li for valuable advice about vertical farming. We thank Rui Yang, Jiahuang Qiu and Tinghui Lyu for assistance with plant care in the hydroponic vertical farms. We thank all members of the Xu laboratory, especially Nan Xiao, Shudong Chen, Yueting Zhang, Yuyuan Lyu and Xu Gao, for assistance with data collection, hydroponic cultivation and plant material acquisition. This research was supported by the Cooperation Project of China, the Netherlands (CAS-NWO) (151111KYSB20210001), the CAS Project for Young Scientists in Basic Research (YSBR-078), and the National Natural Science Foundation of China (32225045) to C.X.

CONFLICTS OF INTEREST

The authors are named as inventors on patents and patent applications related directly to this technology.

AUTHOR CONTRIBUTIONS

C.X. and F.C. designed the experiments, supervised the study, and revised the manuscript. X.Y., Z.L., and Y.Y. performed most of the research and drafted the manuscript. S.L. and Yezi L. performed partial experiments. Yang L. and X.Z. provided technical assistance in hydroponic experiments. All authors read and approved its content.

Edited by: Zhaobo Lang, Southern University of Science and Technology, China

Received Feb. 20, 2025; **Accepted** Apr. 9, 2025

REFERENCES

Brooks, C., Nekrasov, V., Lippman, Z. B., and Van Eck, J. (2014). Efficient gene editing in tomato in the first generation using the clustered regularly interspaced short palindromic repeats/CRISPR-associated9 system. Plant Physiol. **166:** 1292–1297.

Cao, K., Yan, F., Xu, D., Ai, K., Yu, J., Bao, E., and Zou, Z. (2018). Phytochrome B1-dependent control of SP5G transcription is the basis of the night break and red to far-red light ratio effects in tomato flowering. BMC Plant Biol. **18:** 158.

Carrera, E., Bou, J., García-Martínez, J.L., and Prat, S. (2000). Changes in GA 20-oxidase gene expression strongly affect stem length, tuber induction and tuber yield of potato plants. Plant J. **22:** 247–256.

Cheng, M.C., Kathare, P.K., Paik, I., and Huq, E. (2021). Phytochrome signaling networks. Annu. Rev. Plant Biol. **72:** 217–244.

Chory, J., Nagpal, P., and Peto, C.A. (1991). Phenotypic and genetic analysis of det2, a New mutant that affects light-regulated seedling development in Arabidopsis. Plant Cell **3:** 445–459.

Clouse, S.D., Langford, M., and McMorris, T.C. (1996). A brassinosteroid-insensitive mutant in *Arabidopsis thaliana* exhibits multiple defects in growth and development. Plant Physiol. **111:** 671–678.

Coles, J.P., Phillips, A.L., Croker, S.J., García-Lepe, R., Lewis, M.J., and Hedden, P. (1999). Modification of gibberellin production and plant development in Arabidopsis by sense and antisense expression of gibberellin 20-oxidase genes. Plant J. **17:** 547–556.

Daum, T. (2021). Farm robots: Ecological utopia or dystopia? Trends Ecol. Evol. **36:** 774–777.

Eshed, Y., and Lippman, Z.B. (2019). Revolutions in agriculture chart a course for targeted breeding of old and new crops. Science **366:** eaax0025.

Hedden, P. (2003). The genes of the Green Revolution. Trends Genet. **19:** 5–9.

Jansson, S. (1994). The light-harvesting chlorophyll a/b-binding proteins. Biochim. Biophys. Acta **1184:** 1–19.

Kim, E.J., and Russinova, E. (2020). Brassinosteroid signalling. Curr. Biol. **30:** R294–R298.

Kozai, T., and Niu, G. (2016). Plant factory as a resource-efficient closed plant production system. Plant Fact. **4:** 69–90.

Kwon, C.-T., Heo, J., Lemmon, Z.H., Capua, Y., Hutton, S.F., Van Eck, J., Park, S.J., and Lippman, Z.B. (2020). Rapid customization of Solanaceae fruit crops for urban agriculture. Nat. Biotechnol. **38:** 182–188.

Li, T., Yang, X., Yu, Y., Si, X., Zhai, X., Zhang, H., Dong, W., Gao, C., and Xu, C. (2018). Domestication of wild tomato is accelerated by genome editing. Nat. Biotechnol. **36:** 1160–1163.

Liu, F., Song, Q., Zhao, J., Mao, L., Bu, H., Hu, Y., and Zhu, X.G. (2021). Canopy occupation volume as an indicator of canopy photosynthetic capacity. New Phytol. **232:** 941–956.

Lou, H., Li, S., Shi, Z., Zou, Y., Zhang, Y., Huang, X., Yang, D., Yang, Y., Li, Z., and Xu, C. (2025). Engineering source-sink relations by prime editing confers heat-stress resilience in tomato and rice. Cell **188:** 530–549.e520.

Mahadevan, M., Noel, J.K., Umesh, M., Santhosh, A.S., and Suresh, S. (2024). Climate change impact on water resources, food production and agricultural practices. In The Climate-Health-Sustainability Nexus: Understanding the Interconnected Impact on

Populations and the Environment, Singh P., Yadav N., eds, (Cham: Springer Nature Switzerland), pp. 207–229.

Mori, M., Nomura, T., Ooka, H., Ishizaka, M., Yokota, T., Sugimoto, K., Okabe, K., Kajiwara, H., Satoh, K., Yamamoto, K., et al. (2002). Isolation and characterization of a rice dwarf mutant with a defect in brassinosteroid biosynthesis. Plant Physiol. **130:** 1152–1161.

Morita, R., Sugino, M., Hatanaka, T., Misoo, S., and Fukayama, H. (2015). CO_2-responsive CONSTANS, CONSTANS-like, and time of chlorophyll a/b binding protein Expression1 protein is a positive regulator of starch synthesis in vegetative organs of rice. Plant Physiol. **167:** 1321–1331.

Muluneh, M.G. (2021). Impact of climate change on biodiversity and food security: A global perspective—A review article. Agric. Food Secur. **10:** 36.

Ndreca, B., Huttly, A., Bibi, S., Bayon, C., Lund, G., Ham, J., Alarcón-Reverte, R., Addy, J., Tarkowská, D., Pearce, S., et al. (2024). Stacked mutations in wheat homologues of rice SEMI-DWARF1 confer a novel semi-dwarf phenotype. BMC Plant Biol. **24:** 384.

Oikawa, T., Koshioka, M., Kojima, K., Yoshida, H., and Kawata, M. (2004). A role of OsGA20ox1, encoding an isoform of gibberellin 20-oxidase, for regulation of plant stature in rice. Plant Mol. Biol. **55:** 687–700.

Olimpieri, I., Caccia, R., Picarella, M.E., Pucci, A., Santangelo, E., Soressi, G.P., and Mazzucato, A. (2011). Constitutive co-suppression of the GA 20-oxidase1 gene in tomato leads to severe defects in vegetative and reproductive development. Plant Sci. **180:** 496–503.

Pattison, R.J., Csukasi, F., Zheng, Y., Fei, Z., van der Knaap, E., and Catalá, C. (2015). Comprehensive tissue-specific transcriptome analysis reveals distinct regulatory programs during early tomato fruit development. Plant Physiol. **168:** 1684–1701.

Peng, J., Richards, D.E., Hartley, N.M., Murphy, G.P., Devos, K.M., Flintham, J.E., Beales, J., Fish, L.J., Worland, A.J., Pelica, F., et al. (1999). "Green revolution" genes encode mutant gibberellin response modulators. Nature **400:** 256–261.

Pnueli, L., Carmel-Goren, L., Hareven, D., Gutfinger, T., Alvarez, J., Ganal, M., Zamir, D., and Lifschitz, E. (1998). The SELF-PRUNING gene of tomato regulates vegetative to reproductive switching of sympodial meristems and is the ortholog of CEN and TFL1. Development **125:** 1979–1989.

Qin, X., Liu, J.H., Zhao, W.S., Chen, X.J., Guo, Z.J., and Peng, Y.L. (2013). Gibberellin 20-oxidase gene OsGA20ox3 regulates plant stature and disease development in rice. Mol. Plant Microbe. Interact. **26:** 227–239.

Rathor, A.S., Choudhury, S., Sharma, A., Nautiyal, P., and Shah, G. (2024). Empowering vertical farming through IoT and AI-driven technologies: A comprehensive review. Heliyon **10:** e34998.

Richards, D.E., King, K.E., Ait-Ali, T., and Harberd, N.P. (2001). HOW GIBBERELLIN REGULATES PLANT GROWTH AND DEVELOPMENT: A molecular genetic analysis of gibberellin signaling. Annu. Rev. Plant Physiol. Plant Mol. Biol. **52:** 67–88.

Sakamoto, T., Miura, K., Itoh, H., Tatsumi, T., Ueguchi-Tanaka, M., Ishiyama, K., Kobayashi, M., Agrawal, G.K., Takeda, S., Abe, K., et al. (2004). An overview of gibberellin metabolism enzyme genes and their related mutants in rice. Plant Physiol. **134:** 1642–1653.

Sasaki, A., Ashikari, M., Ueguchi-Tanaka, M., Itoh, H., Nishimura, A., Swapan, D., Ishiyama, K., Saito, T., Kobayashi, M., Khush, G.S., et al. (2002). Green revolution: A mutant gibberellin-synthesis gene in rice. Nature **416:** 701–702.

SharathKumar, M., Heuvelink, E., and Marcelis, L.F.M. (2020). Vertical farming: moving from genetic to environmental modification. Trends Plant Sci. **25:** 724–727.

Shohat, H., Cheriker, H., Kilambi, H.V., Eliaz, N.I., Blum, S., Amsellem, Z., Tarkowská, D., Aharoni, A., Eshed, Y., and Weiss, D. (2021). Inhibition of gibberellin accumulation by water deficiency promotes fast and long-term "drought avoidance" responses in tomato. New Phytol. **232:** 1985–1998.

Soyk, S., Müller, N.A., Park, S.J., Schmalenbach, I., Jiang, K., Hayama, R., Zhang, L., Van Eck, J., Jiménez-Gómez, J.M., and Lippman, Z.B. (2017). Variation in the flowering gene SELF PRUNING 5G promotes day-neutrality and early yield in tomato. Nat. Genet. **49:** 162–168.

Su, S., Hong, J., Chen, X.F., Zhang, C.Q., Chen, M.J., Luo, Z.J., Chang, S.W., Bai, S.X., Liang, W.Q., Liu, Q.Q., et al. (2021). Gibberellins orchestrate panicle architecture mediated by DELLA-KNOX signalling in rice. Plant Biotechnol. J. **19:** 2304–2318.

Suganami, M., Suzuki, Y., Tazoe, Y., Yamori, W., and Makino, A. (2021). Co-overproducing Rubisco and Rubisco activase enhances photosynthesis in the optimal temperature range in rice. Plant Physiol. **185:** 108–119.

Tian, J., Wang, C., Chen, F., Qin, W., Yang, H., Zhao, S., Xia, J., Du, X., Zhu, Y., Wu, L., et al. (2024). Maize smart-canopy architecture enhances yield at high densities. Nature **632:** 576–584.

van Delden, S.H., SharathKumar, M., Butturini, M., Graamans, L.J.A., Heuvelink, E., Kacira, M., Kaiser, E., Klamer, R.S., Klerkx, L., Kootstra, G., et al. (2021). Current status and future challenges in implementing and upscaling vertical farming systems. Nat. Food **2:** 944–956.

Wang, P., and Grimm, B. (2021). Connecting chlorophyll metabolism with accumulation of the photosynthetic apparatus. Trends Plant Sci. **26:** 484–495.

Xiao, J.H., Li, H.X., Zhang, J.H., Chen, R.G., Zhang, Y.Y., Ouyang, B., Wang, T.T., and Ye, Z.B. (2006). Dissection of GA 20-oxidase members affecting tomato morphology by RNAi-mediated silencing. Plant Growth Regul. **50:** 179–189.

Yamaguchi, S. (2008). Gibberellin metabolism and its regulation. Annu. Rev. Plant Biol. **59:** 225–251.

Yamamuro, C., Ihara, Y., Wu, X., Noguchi, T., Fujioka, S., Takatsuto, S., Ashikari, M., Kitano, H., and Matsuoka, M. (2000). Loss of function of a rice brassinosteroid insensitive1 homolog prevents internode elongation and bending of the lamina joint. Plant Cell **12:** 1591–1606.

Yeager, A.F. (1927). Determinate growth in the tomato. J. Hered. **18:** 263–265.

Zhang, J., Zhang, X., Chen, R., Yang, L., Fan, K., Liu, Y., Wang, G., Ren, Z., and Liu, Y. (2020). Generation of transgene-free semidwarf maize plants by gene editing of Gibberellin-Oxidase20-3 Using CRISPR/Cas9. Front. Plant Sci. **11:** 1048.

Zhang, L., Yang, X., Li, T., Gan, R., Wang, Z., Peng, J., Hu, J., Guo, J., Zhang, Y., Li, Q., et al. (2022). Plant factory technology lights up urban horticulture in the post-coronavirus world. Hortic. Res. **9:** ubac018.

Zhu, X.-G., and Marcelis, L. (2023). Vertical farming for crop production. Mod. Agric. **1:** 13–15.

SUPPORTING INFORMATION

Additional Supporting Information may be found online in the supporting information tab for this article: http://onlinelibrary.wiley.com/doi/10.1111/jipb.13927/suppinfo

Figure S1. Identification of tomato SlGA20ox and representative phenotypes of *slga20ox1* and *slga20ox2* in solar greenhouse

Figure S2. Diagram of different planting densities in a hydroponic module of vertical farm

Figure S3. Representative phenotypes of *slga20ox1* and *slga20ox2* in a commercial vertical farm

Figure S4. Representative phenotypes of *slga20ox1* and *slga20ox2* in vertical farming (VF) under 0.0255 m^3 space
Figure S5. Representative phenotypes of *slga20ox1* and *slga20ox2* in vertical farming (VF) under a 0.0144 m^3 space with a 60% reduction in lighting power
Figure S6. The verified null mutation alleles and representative phenotypes of *sp sp5g*
Figure S7. Representative phenotypes of *sp sp5g*, *sp sp5g slga20ox1*, and *sp sp5g slga20ox2* in a vertical farm
Table S1. Production efficiency-related phenotypes of different genotypes in the commercial vertical farm
Table S2. Primer sequence
Table S3. Accession numbers

Scan the QR code to view JIPB on WeChat (WeChat: **jipb1952**)

Scan the QR code to view JIPB on X (X: **@JIPBio**)

Scan the QR code to view JIPB on Bluesky (Bluesky: **jipb.bsky.social**)